DEPARTMENT OF DEFENCE
DEFENCE SCIENCE & TECHNOLOGY ORGANISATION
DSTO

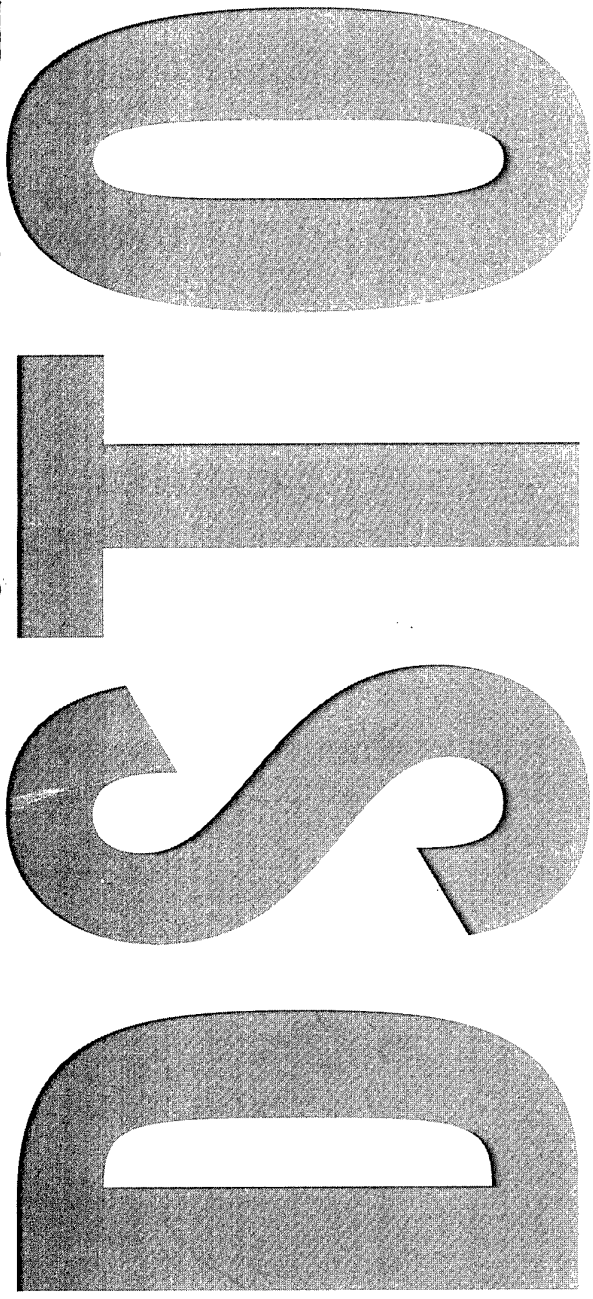

Implementation of a Unified Constitutive Model into the ABAQUS Finite Element Package

R.J. Wescott, K.C. Watters
and M. Heller

DSTO-TR-0833

Implementation of a Unified Constitutive Model into the ABAQUS Finite Element Package

R.J. Wescott, K.C. Watters and M. Heller

Airframes and Engines Division
Aeronautical and Maritime Research Laboratory

DSTO-TR-0833

ABSTRACT

Unified constitutive models have previously been developed at AMRL and implemented into the PAFEC and ABAQUS Finite Element packages to predict the stress-strain response of structures that undergo multi-axial, rate dependent, cyclic plasticity. In this work, the ABAQUS version of the model has been enhanced to account for advances in unified constitutive modelling, and for consistency with the existing PAFEC version of the model. Numerous test cases have been run to validate the model's implementation in ABAQUS. A full 3-dimensional analysis of a proposed test specimen has been undertaken to study residual stress distribution with the ultimate goal of helping to manage fatigue crack growth in the F-111 aircraft.

RELEASE LIMITATION

Approved for public release

DEPARTMENT OF DEFENCE
DEFENCE SCIENCE & TECHNOLOGY ORGANISATION
DSTO

Published by

DSTO Aeronautical and Maritime Research Laboratory
PO Box 4331
Melbourne Victoria 3001 Australia

Telephone: (03) 9626 7000
Fax: (03) 9626 7999

AR-011-003

June 1999

APPROVED FOR PUBLIC RELEASE

Implementation of a Unified Constitutive Model into the ABAQUS Finite Element Package

Executive Summary

High strength D6ac steel is used in the F-111 aircraft for structural components that undergo high stresses. Despite D6ac steel's high strength, some loading conditions on the aircraft are severe enough to cause localised yielding. Yielding of the material leaves residual stresses, which can lead to fatigue cracking under normal service loads. Management of the structural integrity of the F-111 requires knowledge of the crack growth rate behaviour at critical locations in the aircraft. Classical plasticity modelling techniques have been shown to have limitations in predicting material response under non-symmetric cyclic loading. Consequently, over the last decade, AMRL has researched and developed a unified constitutive model to better predict the residual stress field after a Cold Proof Load Test (CPLT) load cycle.

Unified constitutive models have previously been developed at AMRL and implemented into the PAFEC and ABAQUS Finite Element packages to predict the stress-strain response of structures that undergo multi-axial, rate dependent, cyclic plasticity. In this work, the ABAQUS version of the model has been enhanced to account for advances in unified constitutive modelling, and for consistency with the existing PAFEC version of the model. Numerous test cases have been run to validate the model's implementation in ABAQUS. A full 3-dimensional analysis of a proposed test specimen has been undertaken to study residual stress distribution with the ultimate goal of helping to manage fatigue crack growth in the F-111 aircraft.

The result of the work reported herein is the implementation and validation of the best available material model for D6ac steel in the preferred nonlinear Finite Element package ABAQUS. The successful numerical analysis of a proposed test specimen shows that an experimental program should be undertaken.

Authors

R.J.Wescott
Airframes and Engines Division

Ron Wescott graduated from the University of Melbourne in 1973 as a B. Eng (Civil) with First Class Honours. In 1981 he was awarded a PhD from the same university, where his research work involved the development of a finite element method for the geometrically and materially nonlinear analysis of rigid-jointed frames. He has spent more than ten years in industry developing, maintaining and using computer-aided engineering and mining systems. He has had five years experience in the automotive industry using commercial finite element packages to analyse designs of car seat components. He is currently a contractor in the Airframes and Engines Division at AMRL.

K.C.Watters
Airframes and Engines Division

Mr Watters graduated from the University of Sydney in 1973 with a Bachelor of Engineering (Aeronautical) degree. He obtained a Master of Engineering Science degree from Melbourne University in 1981. Mr Watters worked at the Royal Australian Air Force (RAAF) Aircraft Research and Development Unit (ARDU) as a Flight Trials Engineer from 1973 to 1977. He then joined AMRL where he has worked for over 20 years in the areas of vulnerability and lethality studies, experimental stress analysis, structural testing and F-111 Structural Integrity. Mr Watters is currently Head of Structural Testing and Head of F-111 Structural Integrity in AED.

M.Heller
Airframes and Engines Division

Manfred Heller completed a B. Eng. (Hons.) in Aeronautical Engineering at the University of New South Wales in 1981. He commenced employment in Structures Division at the Aeronautical Research Laboratory in 1982. He was awarded a Department of Defence Postgraduate Cadetship in 1986, completing a PhD at Melbourne University in 1989. His work has focussed on the areas of stress analysis, fracture mechanics and fatigue life extension methodologies. Since 1992 he has led tasks which develop and evaluate techniques for extending the fatigue life of ADF aircraft components. He is currently a Senior Research Scientist in the Airframes and Engines Division, Aeronautical and Maritime Research Laboratory, DSTO.

Contents

1. Introduction

Many of the highly stressed structural components in the F-111 aircraft are made of high strength D6ac steel. Nonetheless, for some of these components some infrequent high loading conditions on the aircraft are sufficient to cause yielding of the material, particularly around stress concentrators such as holes. The yielding of the material leaves tensile residual stresses, which can cause fatigue cracking under subsequent normal service loads. It has been found in both RAAF[1] and USAF[2] service of the F-111 that fatigue cracks have developed at these yielded locations and have grown through the yield zone and residual stress field. The main loading condition causing this yielding is the Cold Proof Load Test (CPLT), in which the aircraft is subject to limit load cycles in a ground test rig. This test is performed at regular intervals and is the cornerstone of the safety-by-inspection program for the D6ac steel components in the aircraft. CPLT involves the application of two cycles of negative and positive limit loads at two wing sweep angles as follows: @ 56° wing sweep, $0 \rightarrow -2.4\ g \rightarrow 0 \rightarrow +7.33\ g \rightarrow 0$; @ 26° wing sweep $0 \rightarrow -3.0\ g \rightarrow 0 \rightarrow +7.33\ g \rightarrow 0$.

Cyclic yielding induced by these two CPLT load cycles is complex to analyse. Finite Element Analysis (FEA) provides a powerful means of predicting materially nonlinear response in complex structures undergoing cyclic loading. However, the disadvantages of classical plasticity models used in FEA to simulate inelastic cyclic response led AMRL to investigate other constitutive models. State variable constitutive models offer more accurate predictions of strain rate and cyclic response effects. The state-variable based constitutive model used at AMRL for modelling inelastic response of D6ac steel was initially developed by Stouffer and Bodner [1] and Ramaswamy [2], and has subsequently been jointly enhanced by AMRL, The University of Melbourne and Monash University[3]. The model, referred to as the unified constitutive model, has been implemented into the PAFEC Finite Element package [3], which was the only relevant package available at the time.

Whilst PAFEC has facilities for nonlinear analysis, and will allow the installation of user material models, the ABAQUS Finite Element package has developed a wide reputation as the preferred nonlinear finite element code. Indeed, MacNeal-Schwendler Corporation, the developers of NASTRAN, markets and recommends ABAQUS for nonlinear analysis. Also, the current PAFEC implementation of the unified constitutive model requires modifying more than 20 existing PAFEC routines as well as creating more than 30 new routines. Hence, limitations of the PAFEC implementation are the time and expertise required maintaining the unified constitutive model when new versions of PAFEC are released. Therefore, when ABAQUS became available, an implementation of the unified constitutive model into that package was desirable.

---

[1] Royal Australian Air Force.

[2] United States Air Force.

[3] Reference [3] contains more information on the history of the model's development.

This report describes the implementation of the Ramaswamy-Stouffer-Bodner unified constitutive model into ABAQUS, which was based on development work done by Monash University [4]. Section 2 discusses limitations of existing ABAQUS plasticity models, gives the mathematical background of the unified constitutive model, and describes the implementation of the model into ABAQUS, noting differences from previous work [4]. Section 3 describes a proposed test specimen, and details preliminary (elastic) finite element modelling of the specimen. In Section 4 an elasto-plastic analysis of the specimen is reported, with the aim of characterising the fatigue crack growth through a residual stress field left after yield of a D6ac component.

2. Constitutive Modelling Approach

2.1 Existing ABAQUS Plasticity Models

ABAQUS has several options for plasticity models [5] that are applicable to the inelastic behaviour of metals. Most of these models are incremental, in that the total strain is separated into an elastic part, on which all changes in stress depend, and a plastic part. Incremental plasticity models generally are defined by the following: (i) a yield function, (ii) a flow rule, and (iii) a hardening law.

ABAQUS has two yield criteria suitable for predicting behaviour of metals, viz., (i) Von Mises criterion, and (ii) Hill criterion, which is a form of the Von Mises function that allows for anisotropic response. The ABAQUS material models for plasticity adopt associative flow rules, viz. plastic straining is normal to the yield surface. ABAQUS allows for perfectly plastic response, isotropic hardening and kinematic hardening, and has a nonlinear isotropic/kinematic hardening model which is intended to model the cyclic loading of metals. Strain rate effects can be accounted for in ABAQUS's simple isotropic hardening scheme, but are not available for kinematic hardening and combined isotropic/kinematic hardening.[4] Creep models are available in ABAQUS, but these are not applicable to creep under cyclic loading. Also, if creep and plasticity occur simultaneously, the response may not be predicted correctly.

Plasticity in ABAQUS is one of a range of nonlinear material behaviours that can be simulated. The general approach in ABAQUS to the solution of nonlinear problems is to apply the loading in steps, with the load in each step being divided into increments. Equations representing the response of the structure to a load increment are solved by iteration - the Newton-Raphson method (and variations) is adopted, with judicious monitoring of progress towards convergence to ensure a computationally efficient

[4] When strain rate effects are negligible, ABAQUS's combined isotropic/kinematic hardening (nonlinear kinematic hardening) model may provide an efficient alternative to the Unified Constitutive Model.

solution. After a material point has yielded, its stress components are updated for the increment using an implicit integration scheme.

A powerful feature of the ABAQUS Finite Element Package is the ability to include a users constitutive model through the UMAT facility.

2.2 The Unified Constitutive Model - Background

As shown in the previous section, ABAQUS plasticity modelling has several disadvantages, in common with all classical techniques. Unified constitutive models offer improved representation of strain rate and cyclic response effects [6], which means time dependent responses such as creep, stress relaxation and cyclic hardening/softening can be predicted with greater accuracy.

Unified constitutive models[5] are so-called because classical plastic strain and creep strain are 'unified' into a single inelastic strain ε_{ij}^{I}. This, by definition, overcomes the problems of classical plasticity when plasticity and creep occur together. Also, with no distinction between plasticity and creep regimes, high and low temperature responses are simulated with the same set of basic equations. Thus, in isothermal applications, the total strain (ε_{ij}) is,

$$\varepsilon_{ij} = \varepsilon_{ij}^{E} + \varepsilon_{ij}^{I} \tag{1}$$

where ε_{ij}^{E} is the elastic strain. The total stress (σ_{ij}) is defined by,

$$\sigma_{ij} = C_{ijkl} . \varepsilon_{ij}^{E} \tag{2}$$

where C_{ijkl} is the (constant) elastic constitutive tensor. In the displacement-based finite element method, total strains are available at each stage of the solution. The major function of a unified constitutive model is to predict the values of inelastic strain, from which elastic strain and total stress can be determined. Inelastic strain is modelled (in rate form) as a function of deviatoric stress (S_{ij}) and two state variables, back stress (Ω_{ij}), and drag stress (Z). Back stress is a tensor quantity that represents, at microscopic level, dislocation movements and pile-ups. Drag stress is a scalar that models the evolution of subgrains and other orientation-independent microscopic properties. The inelastic flow equation of the unified constitutive model developed initially by Stouffer and Bodner [1] and Ramaswamy [2] is:

$$\dot{\varepsilon}_{ij}^{I} = D \exp\left[-\frac{1}{2}\left(\frac{Z^2}{3K_2} \right)^{n} \right] \frac{\left(S_{ij} - \Omega_{ij} \right)}{\sqrt{K_2}} \tag{3}$$

[5] The background to the unified constitutive model detailed in this section follows the description given by Trippit [7].

where $\dot{\varepsilon}_{ij}^{I}$ is the inelastic strain rate, D and n are temperature and strain rate dependent material parameters, and K_2 is the second invariant of the over stress tensor $(O_{ij} = S_{ij} - \Omega_{ij})$, viz.,

$$K_2 = \frac{1}{2}(S_{ij} - \Omega_{ij}).(S_{ij} - \Omega_{ij}) \tag{4}$$

The deviatoric stress (S_{ij}) is defined by,

$$S_{ij} = \sigma_{ij} - \delta_{ij}\sigma_m \tag{5}$$

where δ_{ij} is the Kronecker delta, and σ_m is the mean (or hydrostatic) stress, viz.,

$$\sigma_m = \frac{1}{3}(\sigma_{11} + \sigma_{22} + \sigma_{33}) \tag{6}$$

In Equation (3), for D6ac steel at room temperature, D = 10 000 for tensile and fatigue loadings (strain rates up to 1.0 sec $^{-1}$), and n = 3 to model the strain rate insensitivity of the response. The inelastic flow equation (Eqn 3) requires values of back stress. Several forms of the back stress evolution equation have been proposed for the unified constitutive model. In this development the back stress rate $(\dot{\Omega}_{ij})$ is defined by the multi-axial stress form of an equation derived by Trippit [7], p.79,

$$\dot{\Omega}_{ij} = \frac{2}{3} f_1 \Omega_{ss} \dot{\varepsilon}_{ij}^{I} - f_1 \dot{\varepsilon}_{equ}^{I} \Omega_{ij} + f_2 \dot{S}_{ij} \tag{7}$$

where f_1 is a hardness related material parameter, Ω_{ss} is the steady state value of back stress[6], f_2 is another material parameter, $\dot{\varepsilon}_{equ}^{I}$ is the equivalent inelastic strain rate and $\dot{S}_{ij}$ is the deviatoric stress rate. The equivalent inelastic strain rate is defined as :

$$\dot{\varepsilon}_{equ}^{I} = \sqrt{\frac{2}{3}\dot{\varepsilon}_{ij}^{I}\dot{\varepsilon}_{ij}^{I}} \tag{8}$$

Also required for the evaluation of inelastic strain rates is the drag stress (Z). Its evolution equation is :

$$Z = Z_1 + (Z_0 - Z_1)\exp(-m\varepsilon_{equ}^{I}) \tag{9}$$

where Z_0 and Z_1 are initial and final values of drag stress, m controls the rate at which Z evolves from Z_0 to Z_1, and ε_{equ}^{I} is the equivalent inelastic strain. Z_0, Z_1 and m are material parameters, and, from Equation (8), ε_{equ}^{I} is given by:

$$\varepsilon_{equ}^{I} = \int \sqrt{\frac{2}{3}\dot{\varepsilon}_{ij}^{I}\dot{\varepsilon}_{ij}^{I}}\, dt \tag{10}$$

---

[6] Ω_{ss} is also referred to as 'equilibrium back stress' or 'saturated back stress' [6]. For tensile and fatigue response, $\Omega_{ss} = \Omega_{max}$, the maximum back stress reached at inelastic saturation.

Equations (3), (7) and (8) form a system of ordinary differential equations (ODEs), the solutions of which yield components of inelastic strain and back stress, as well as the equivalent inelastic strain. The Livermore Solver [8] has proved to be very effective in the solution of the unified constitutive model ODEs [7], and is used in this implementation of the model. Searl and Paul [9] have derived values for the material parameters $f_1, f_2, \Omega_{max} (\equiv \Omega_{ss}), Z_0, Z_1$ and m for D6ac steel.

2.3 The Unified Constitutive Model - Implementation

The unified constitutive model has previously been implemented at AMRL in the PAFEC finite element package [3]. That implementation is part of work on the Ramaswamy-Bodner-Stouffer version of the unified constitutive model that has been carried out at AMRL and elsewhere over the past ten years[7]. The PAFEC implementation of the model for D6ac steel involved new routines for automatic time step load calculation and structural convergence control, as well as routines to model material behaviour. However, ABAQUS is able to completely manage the solution process at the structural level. Hence, this implementation only required the development of UMAT (User Material) modules to calculate total stress and a consistent Jacobean matrix for a material point. Monash University was contracted to implement the unified constitutive model developed at AMRL into ABAQUS [4]. The implementation presented herein is based on that work.

Several modifications have been made to the Monash version for the current ABAQUS installation, the main purposes being to update the model in accord with advances in unified constitutive modelling, and to produce a material model which will give results consistent with equivalent PAFEC analyses. The back stress evolution equation has been updated. The previously used one was (compare to Eqn 7):

$$\dot{\Omega}_{ij} = f_1 \dot{\varepsilon}^I_{ij} - \frac{3}{2} \frac{f_1}{\Omega_{ss}} \dot{\varepsilon}^I_{equ} \Omega_{ij} + f_2 \dot{S}_{ij} \qquad (11)$$

A measure of effective inelastic strain is required in the drag stress evolution equation (Eqn 9). The previous implementation used a different definition of effective inelastic strain, viz., the inelastic strain magnitude (ε^I_{eff}), which is defined by,

$$\varepsilon^I_{eff} = \sqrt{\frac{2}{3} \varepsilon^I_{ij} \varepsilon^I_{ij}} \qquad (12)$$

The drag stress should evolve during loading by *asymptoting* to a saturated value. However, during cyclic loading the inelastic strain magnitude will increase, then decrease and increase again, resulting in *fluctuating* values of drag stress. The previous formulation prevented the fluctuation by modifying the application of the drag stress equation. However, equivalent plastic strain (Eqn 10), which is used in the current PAFEC (L8.1) code, monotonically increases during loading. Adopting this definition of equivalent inelastic strain results in a more general, more efficient and simpler-to-use formulation,

[7] Searl and Paul's report [9] contains a comprehensive list of references on the development of the model and its implementation into PAFEC at AMRL.

because strain softening can be modelled, fewer state variables are needed, and Initial Conditions are no longer needed in the ABAQUS input deck (for tension and fatigue loadings). Other modifications are an increase in the number of ABAQUS element types that can use the material model (Section 2.4), and the facility to analyse a model containing more than one element type.

2.4 Supported Element Types

The ABAQUS user material interface provides the numbers of direct stresses and shear stresses as input to the user-written constitutive model. In the most general case, there are three direct stresses and three independent shear stresses at a material point. However, most element types do not require the full set. Hence the constitutive model should be developed for variations in the number of stresses. This implementation of the unified constitutive model supports all Version 5.6 ABAQUS elements with displacement degrees-of-freedom, as summarised in Table 1.

2.5 Validation

2.5.1 Introduction

It is necessary to verify that the implementation of the unified constitutive model into ABAQUS is performing as expected. One, two and three-dimensional test cases have been created to prove the implementation - these tests are similar to the suite developed to validate the installation of the model into PAFEC [3]. In both instances the test case results have been compared to output from a standalone FORTRAN program which simulates uniaxial response. A description of this program, which is named TREACLE, is given in Appendix A. The application of the unified constitutive model to D6ac steel has been validated by Searl and Paul [9], where appropriate material constants have been determined, and experimental test data and numerical results compared.

2.5.2 Description of Test Cases

The test cases used element types that encompassed all relevant variations of direct and shear stresses, as outlined in Table 1. Tests also involved a variety of loadings and different configurations of elements. The loading types were uniaxial pull, constrained pull, shear and uniaxial cyclic. Element shapes were cubic, square or linear, with a constant element edge length of 1 mm.

Table 1. Summary of Supported Element Types

Element type	Number of direct stresses	Number of independent shear stresses
3D Solid	3	3
Plane Strain	3	1
Plane Stress, Shells, Axisymmetric shells with non-axisymmetric loading, Elbows	2	1
Axisymmetric shells	2	0
Beams with torsional shear stress	1	1
Truss, Beams without torsional shear stress	1	0

Tables 2, 3 and 4 give a summary of these test cases with the types of elements and loading conditions that have been validated. In test cases where the response was uniaxial and uniform the solutions were compared to answers from the TREACLE program. In all tests, criteria involving stress and strain values were invoked for validating the test results. In Tables 2 and 3 the test case numbers 1-13 perform the same verifications as the corresponding PAFEC tests [3]. Cases 14-17 are further tests. Material constants adopted in the test cases were the same as those used in the PAFEC validation [3], viz.,

Ω_{max}	= 1250 MPa	Z_0	= 250 MPa
m	= 9	Z_1	= 550 MPa
E	= 207 GPa	f_1	= 72
ν	= 0.32	f_2	= 0.68

The maximum inelastic strain rate (D) and strain rate sensitivity parameter (n) have the values defined in Section 2.2. Figure 1 is the typical stress-strain curve for the aforementioned data, to 40 000 $\mu\varepsilon$ at a strain rate of 100 $\mu\varepsilon$ sec^{-1}. The data points of which were generated using TREACLE , which is described in Appendix A.

Table 2. Summary of Test Cases with 3-Dimensional Elements

Test no.	Data file	Element type	Element configu-ration	Loading condition	Description
1	A3D1	C3D20R	2x2x2	Free Uniaxial Pull	Test the general stress to strain response.
2	A3D2	C3D20R	2x2x2	Constrained Pull	Test the general stress to strain response under different hydrostatic conditions than test 1.
3	A3D3	C3D8R	1	Shear	Test the general stress to strain response in shear.
4	A3D4	C3D20R	2x2x2	Free Uniaxial Cyclic	Test the cyclic stress to strain response.

Table 3. Summary of Test Cases with 2-Dimensional Elements

Test no.	Data file	Element type	Element configu-ration	Loading condition	Description
5	APS1	CPS8	2x2	Free Uniaxial Pull	Plane stress. Test the general stress to strain response.
6	APS2	CPS8	2x2	Constrained Pull	Plane stress. Test the general stress to strain response under different hydrostatic conditions than test 5.
7	APS3	CPS4	1	Shear	Plane stress. Test the general stress to strain response in shear.
8	APS4	CPS8	2x2	Free Uniaxial Cyclic	Plane stress. Test the cyclic stress to strain response.
9	APE1	CPE8	2x2	Free Uniaxial Pull	Plane strain. Test the general stress to strain response.
10	APE2	CPE4	1	Shear	Plane strain. Test the general stress to strain response in shear.
11	APE3	CPE8	2x2	Free Uniaxial Cyclic	Plane strain. Test the cyclic stress to strain response.
12	ASH1	S8R	2x2	Free Uniaxial Pull	Test the general stress to strain response.
13	AMU1	S8R CPS8 CPE8	1+1+1[8]	Free Uniaxial Pull	Multiple element type tests.
14	ASA1	SAX1	1	Free Uniaxial Pull	Test the general stress to strain response.

[8] One element of each type, not connected to each other, individually loaded.

Table 4. Summary of Test Cases with 1-Dimensional Elements

Test no.	Data file	Element type	Element configu-ration	Loading condition	Description
15	AB1	B31	1	Free Uniaxial Pull	Test the general stress to strain response.
16	AB2	B31	1	Torsion	Test the general stress to strain response in pure torsional loading.
17	AT1	T2D2	1	Free Uniaxial Pull	Test the general stress to strain response.

Two of the test cases are described below. The model for Test 1, which is summarised in Table 2, was a three dimensional block composed of eight 3D continuum elements. The block was loaded by prescribed displacements on four of the element faces, as shown in Figure 2a. Figure 2b shows the block restrained on the faces opposite to the loaded faces, as well as on two adjoining planes, to prevent rigid body motion and preserve uniformity of response. The applied loading caused a maximum strain of 40 000 με. The time of the analysis was 400 sec, giving a constant strain rate of 100 με sec $^{-1}$. Results of this analysis are shown in Figure 3. Test 4, which is summarised in Table 1, had the same finite element configuration, maximum prescribed displacement and restraints as the Test 1, but underwent the cyclic loading shown in Figure 4. Results of this analysis are shown in Figure 5. Results of all tests satisfied criteria for stress and strain, and, where applicable, results agreed with output from the standalone TREACLE program, as shown, for example, in Figures 3 and 5.

3. Elastic Numerical Analysis of Test Specimen

Elastic and inelastic numerical analyses in this study have been performed using the ABAQUS Finite Element Package, Version 5.6, running on a Hewlett-Packard K Series 9000 computer at AMRL. Patran Version 7.5 has been used for all pre- and post-processing. Twenty-noded hexahedral elements have been used for all runs.

3.1 Geometry of Test Specimen

Figure 6 shows the geometry of the test specimen. The specimen is made from D6ac steel bar stock and has outside dimensions 550 by 150 by 30 mm. The middle section has been reduced in thickness to 5 mm, and a 30 mm diameter hole has been drilled in the centre of the plate to act as a stress concentrator. Section A-A in Figure 6 shows that 30 mm wide 'flanges' remain at the edge of the central plate, to give the specimen stability when tested in compression.

3.2 Preliminary Analyses

3.2.1 Introduction

Several preliminary elastic analyses were conducted. The aims of these analyses were to determine the following: (i) the most appropriate way to model the load, (ii) if lateral stability would be a limiting factor when testing in compression, and (iii) what was likely to be an adequate mesh density for detailed analyses. Because none of these aims involved an accurate prediction of the stresses around the hole, the analyses could be carried out with a relatively coarse mesh. However, a refined mesh model would also be needed to obtain accurate estimates of stress for elastic and inelastic cases. To facilitate general refinement of the mesh and to give flexibility in local mesh refinement a blocking scheme was used. Figure 7 shows the blocking scheme for a 1/8-model of the test specimen.

3.2.2 Modelling of Load Application

For investigating the load application, symmetry allows a 1/8-model to be used. Figure 8 shows the model, which has 495 20-noded hexahedral elements, with Young's Modulus equal to 210 GPa, and Poisson's Ratio 0.3. The restraints introduced by modelling $1/8^{th}$ of the test specimen are sufficient to constrain the model against rigid body motion.

The aims of this set of analyses were to determine the following: (i) whether the size of the finite element model could be reduced by neglecting the part of the specimen that would be gripped in the testing machine, (ii) if the contact pressure applied through the grips of the testing machines affected stresses at the hole, and (iii) if the assumed distribution of the tensile/compressive force affected stresses at the hole.

The following five load cases were analysed:

i. Base case - load applied to the end surface (150 mm by 30 mm surface, refer to Figure 6) as a pressure.
ii. Short sample - the 150 mm by 140 mm by 30 mm (refer to Figure 6) portions at the ends of the sample are removed. The load is applied as an 'end pressure', as in the base case.
iii. Contact pressure - load applied to the end surface as a pressure, with the testing machine grips exerting a uniform contact pressure of 30 MPa.
iv. Uniform Shear - load applied to the surfaces of the specimen in contact with the testing machine grips, as a uniformly distributed shear force.
v. Linear Shear - load applied to the surfaces of the specimen in contact with the testing machine grips, as a shear force with a bilinear distribution, viz., at a maximum half way along each grip.

In all cases, the equivalent longitudinal load was 135 kN (or 30 MPa). Table 5 shows values of maximum stress for each load case[9], and the difference from the base result.

Table 5 - Results of Load Application Modelling

Load case	Maximum stress (MPa)	% difference (from (1))
1	369.3	-
2	415.4	+12.5
3	372.0	+0.7
4	369.6	+0.1
5	369.6	+0.1

Specific conclusions from these analyses are the following:

i. the 'short sample' results differ significantly from the base case. Hence, a full-length model must be used.

ii. addition of contact pressure has a minor effect on results (about 0.7%). Therefore, it can be disregarded in modelling.

iii. change in application of load from end pressure to shear force makes little difference (less than 0.10%). Changing the shear force distribution from uniform to bilinear makes no discernible difference.

The general conclusion is that the test specimen should be modelled to full length, with the load applied as an end pressure, and no contact pressure exerted by the grips.

3.2.3 Buckling

The first buckling analysis was done with a full model (3960 elements), so that no buckling modes would be excluded by assumptions of symmetry. Young's Modulus was chosen as 209 GPa, and Poisson's Ratio as 0.3. The critical load that the test specimen could reach was considered to depend greatly on the degree of restraint provided by the jaws of the test machine. It was decided to initially adopt a simple (conservative) assumption for the degree of restraint, and improve modelling of the restraint only if the results were unsatisfactory. The first condition was a 'hinge' at both ends of the specimen. The buckling load predicted by ABAQUS in this case was 376 kN. Because the proposed loads were to exceed 1000 kN, this was not satisfactory.

The lowest three buckling modes were examined for the 'hinged-at-end' case, and they showed that further analysis could reliably be undertaken with a ¼-model of the specimen. This model (which was also modified in a minor way) contained 1032 elements. After confirming that the ¼-model gave the same results as the full model for the 'hinged-at-end' case, a second analysis was done with restraints modelled as hinges halfway along each grip. The buckling load in this case was 589 kN, which was still not

[9] The maximum stresses are predicted at the edge of the hole, nearest the specimen 'flanges', at half-thickness of the plate. They act in the longitudinal direction of the specimen.

enough. Hence, it was necessary to model the degree of restraint more accurately. Discussions with the test engineer concluded that all of the ends of the specimen would be held in the jaws of the test machine, and that its grips would fix the specimen against all rotations as well as translation. The buckling load predicted for this fully fixed option was 2065 kN. Figure 9 shows that the deformation mode is buckling of the 5 mm thick central section. This analysis shows that the test specimen (given correct alignment) could be loaded to approximately 1000 kN without the likelihood of excessive lateral displacements.

3.2.4 Mesh Density

Figure 10 shows the 'maximum differences' in the longitudinal stresses for the base case, in the region of the hole. 'Maximum differences' are calculated by extrapolating longitudinal stresses in an element to its nodes, and comparing the values at each node from all elements which 'use' that node. Hence, it is a measure of the coarseness of the mesh, and can be interpreted as an indication of the mesh error.

The size of the mesh errors showed that the mesh needed some refining. Five elements were used through the half-thickness in the coarse mesh. Because of the relatively small variation in longitudinal stress through the thickness, five elements were considered to be adequate. In the coarse mesh the element densities in the two blocks surrounding the hole (on the 1/8-model) were 3 by 3 and 2 by 3. For the refined mesh it was decided to try 9 by 8 and 6 by 8. In general, element side lengths vary within a block. The element sizing was based on a qualitative assessment of stress gradients for Load Case 1, with, of course, shorter edge lengths where stress gradients are high. The refined mesh 1/8- model of the test specimen contains 1854 elements.

3.3 Analyses with Refined Mesh

The base case in Section 3.1.3 was analysed again with the refined mesh shown in Figure 11. The maximum stress reached was 363.9 MPa (compared to 369.3 MPa in the coarse mesh analysis, a 1.5% difference), although the variation was greater in other areas. Figure 12 shows the 'maximum differences' in the longitudinal stresses in the region around the hole. The highest values in the area of interest are about 2 MPa, from which it can be concluded that the mesh density is adequate. To validate conclusions that were based on the coarse mesh (Section 3.1.3), an analysis was done with a combination of a uniform shear force and a contact pressure (6 MPa) using the refined mesh. The result was a maximum stress of 365.5 MPa, only 0.4% greater than the base case, which confirms the conclusions reached in Section 3.1.3.

4. Elasto-Plastic Numerical Analysis of Test Specimen

4.1 Analysis Using Existing ABAQUS Plasticity

One of the main steps in the proposed experimental program is to load the specimen so that a maximum compressive strain of 20 000 με is reached. Hence, this strain level must be attained in the numerical analysis with the unified constitutive model. The classical plasticity models available in ABAQUS are algorithmically simple in comparison with the unified constitutive model, and therefore analysis using a classical plasticity model is computationally more efficient. Hence, it was decided that an analysis with classical plasticity would be valuable in estimating the load (and its incrementation) to be applied in a unified constitutive model analysis. Also, the results would provide a limited validation of responses predicted by the unified constitutive model, particularly up to initial yield.

The fine finite element model used for elastic analysis was adopted, with reduced integration elements[10]. The plasticity model applied is the Von Mises yield criterion, with Prandl-Reuss flow equations, and no hardening (viz., perfectly plastic behaviour). Young's Modulus (E) is 203 GPa, Poisson's Ratio (ν) is 0.3 and the yield stress is 1460 MPa, which equates to a yield strain of approximately 7200 με. Figure 13 shows the total longitudinal strains at a load of 1012 kN (in compression) predicted by the classical analysis. The total load (1350 kN) was applied in two steps, the first being one increment of 60% of the total load, the second of eight increments of the remaining 40%. Because D6ac steel shows significant strain hardening and this analysis assumes perfectly plastic response, the strains predicted at the load level shown are expected to be higher than those attained in a test. However, it is estimated that the desired strain (20 000 με) would be attained at a load of approximately 1000 kN.

4.2 Analyses Using Unified Constitutive Model

4.2.1 Introduction

The finite element mesh and element type for analyses using the unified constitutive model were the same as for classical plasticity analyses (Section 4.1). The material constants and the loading sequence are described in the following sections.

4.2.2 Constitutive Constants

The material constants adopted in these analyses are based on the constitutive constants derived by Searl and Paul [9, Section 7.2] and are as follows:

Ω_{max} = 1250 MPa $\qquad$ Z_0 = 1081 MPa

[10] The fully integrated form of the ABAQUS 20-noded hexahedral element exhibits volumetric locking when response is incompressible, as occurs for the plasticity model adopted here.

m	= 120	Z_1	= 600 MPa
E	= 205 GPa	f_1	= 135
ν	= 0.32	f_2	= 0.585

Note that the implementation of the unified constitutive model into ABAQUS allows f_1 and f_2 to evolve in a similar manner to the drag stress (Eqn 4). However, here the recommended values for f_1 and f_2 are constant. This can be accomplished by setting the initial and final values of f_1 and f_2 to their constant values, in which case the parameters that would control the evolution of f_1 and f_2 are arbitrary. As mentioned in Section 2.2, the strain rate sensitivity parameter (n) is set to 3.0. Finally, the Jacobean factor, which controls the accuracy of the Jacobean matrix calculated by the model, is set to 3.

4.2.3 Loading Scheme

The loading scheme for numerical analysis was intended to simulate the loading in the Plastic Strain Survey of the proposed CPLT on the specimen. To this end, the model was first analysed in monotonic compression to determine the load which would cause a maximum direct strain of 20 000 με. The result was a load of 1012 kN. The loading scheme for the numerical analysis is as follows, with ten equal increments in all load steps, except the fourth, which has a single increment, because of the relatively small increase from 950 to 1012 kN.

Sequence of loading is as follows:

i. Ramp the load in tension to 310 kN.
ii. Unload to zero load.
iii. Ramp the load in compression to 950 kN.
iv. Ramp the load in compression to 1012 kN.
v. Unload to zero load.
vi. Ramp the load in tension to 414 kN.
vii. Unload to zero load.
viii. Ramp the load in compression to 1012 kN.
ix. Unload to zero load.

The loading rate is a uniform 4.5 kN/sec.

4.2.4 Results

Figure 14 shows total direct strains (longitudinal) at the first maximum load in compression. As for elastic analyses, the maximum strain occurs at the hole edge, nearest to the 'flanges', at half-thickness of the plate. The finite element stress history (Von Mises and longitudinal stresses) at the position of maximum strain is shown in Figure 15 for the CPLT loading cycle. Figure 16 shows the variation of longitudinal stress with longitudinal strain at the maximum strain position for the CPLT loading cycle. Figure 17 shows the residual (longitudinal) stresses in the region of the hole at the completion of the first CPLT cycle (end of Load Step (v)). The maximum occurs at the same place as the maximum total strain, as shown in Figure 14. Residual stresses at the end of the second

CPLT cycle (end of Load Step (ix)) are shown in Figure 18. Comparison of maximum and minimum residual stresses after the first and second CPLT cycles shows an increase in the tensile stress of about 3%, and an increase in compressive stress of about 10%. Examination of Figures 17 and 18 shows that the regions of tensile and compressive residual stress have grown from the first to the second cycle. Figure 19 shows the residual Von Mises stress distribution along the half-width of the specimen at the end of the second CPLT cycle. The distribution is plotted at the free surface of the specimen, at the mid-surface and at ¼-thickness.

5. Conclusions

A Ramaswamy-Bodner-Stouffer version of the unified constitutive model has been successfully implemented into the ABAQUS finite element package. All relevant combinations of numbers of direct stresses and shear stresses have been tested, demonstrating that all ABAQUS (V5.6) element types can use the unified constitutive model. Results from a suite of test cases agreed with answers from TREACLE, the standalone program for running the unified constitutive model. TREACLE, which outputs stress given total strain, was used in prior work to validate results from the PAFEC implementation of the model [3], verifying that the ABAQUS version of the model is consistent with the PAFEC version. Therefore, results from ABAQUS and PAFEC analyses of the same problem can be compared in the knowledge that material behaviour is modelled identically. Documentation for TREACLE has been included in this report.

Elastic analyses of the proposed test specimen have shown that the specimen should be modelled to its full length, with the load applied as an end pressure, and that the contact pressure exerted by the test machine grips can be ignored. An elastic buckling analysis predicted that the correctly aligned and fully restrained specimen could support the proposed test load of about 1000 kN without excessive lateral displacements.

The ABAQUS implementation of the unified constitutive model was successfully applied in the analysis of the proposed test specimen. This showed that the constitutive model could be used in ABAQUS for real problems with a large number of degrees-of-freedom. The residual stresses predicted under simulated CPLT loading verify that the specimen is suitable for experimental testing. It is recommended that an experimental program be undertaken on the specimen, with CPLT loading based on the finite element analysis loading scheme (Section 4.2.3).

6. References

1. **STOUFFER, D.C. and BODNER, S.R.,** *A Relationship Between Theory and Experiment for a State Variable Constitutive Equation,* in 'Mechanical Testing for Deformation Model Development', ASTM STP 765, ASTP, Philadelphia, 239-250, 1982.
2. **RAMASWAMY, V. G.,** *A Constitutive Model for the Inelastic Multiaxial Cyclic Response of a Nickel Based Superalloy René 80,* NASA Contractor Report 3998, July 1986.
3. **PAUL, J.,** *Implementation of a Unified Constitutive Model into the PAFEC Finite Element Package: Final Report,* Aeronautical and Maritime Research Laboratories, TR-0529, DSTO, Melbourne, Aust, May 1997.
4. **SAWYER, J.P.G. and JONES, R.,** *Documentation for an Isotropic Implementation of the Bodner-Stouffer-Ramaswamy "Unified" Constitutive Model in ABAQUS,* Final Report: COE-SM 97-09, June 1998.
5. **HIBBITT, KARLSSON & SORENSEN, INC.,** 1080 Main Street, Pawtucket, RI 02860-4847, *ABAQUS/Standard User's Manual, Version 5.6.*
6. **STOUFFER, D.C. and DAME, L. T.,** *Inelastic Deformation of Metals: Models, Mechanical Properties, and Metallurgy,* John Wiley & Sons Inc., New York, March 1996.
7. **TRIPPIT, B.,** *Development and Implementation of a Unified Constitutive Model for Finite Element Analysis,* Unpublished Ph.D. thesis, Royal Melbourne Institute of Technology, August 1997.
8. **HINDMARSH, A. C.,** *ODEPACK, a systematized collection of ODE solvers.* In R. Stepleman et al., editors, *Scientific Computing, Volume 1,* pages 55-64. IMACS/North-Holland Publishing Company, North-Holland, Amsterdam, 1983.
9. **SEARL, A. and PAUL, J.,** *Characterisation of D6AC Steel Using A Unified Constitutive Model,* Aeronautical and Maritime Research Laboratories, TR-0556, DSTO, Melbourne, Aust, July 1997.

Appendix A: Unified Constitutive Model Standalone Program (TREACLE)

A.1 TREACLE Program

TREACLE is a standalone program which 'runs' the Ramaswamy-Bodner-Stouffer unified constitutive model, in the form described in this report. As input it uses material parameters describing the constitutive properties of the material, and a loading history, which is typically a total strain rate acting over a specified time. The input parameters are used in the unified constitutive model to calculate total stress, state variables and other results. The solution process is controlled by a series of commands read from a command file, the format of which is based on an ABAQUS input deck, viz., command lines beginning with *, comment lines beginning with **, and data lines. User-selected variables are written to a text file at discrete times in the loading history. Finally, plotting software can be run to produce a graphical representation of results from the model.

The primary purpose of TREACLE is to aid in estimating material constants for use in a finite element method implementation of the unified constitutive model, by predicting values of stress/strain variables which can readily be compared to experimental results (eg, [9]). The PERTURB function in TREACLE allows a selected parameter to take a range of values (with other parameters held constant), to assess the effect of varying that parameter. TREACLE is also a tool for validating results from finite element method implementations of the unified constitutive model. For instance, the Uniaxial Stress-Strain Curve in Figure 1, and validation solutions in Figures 3 and 5 were obtained by running TREACLE with the same material constants and total strain rate as the finite element test cases. Figure A.1 contains a list of the names and functions of the routines that make up TREACLE, and Figure A.2 shows the calling hierarchy of the program.

Main Program

TREACLE	Displays banner and opens input command file

Subroutines

INITIAL	Sets initial stresses and strains to zero
INTERP	Reads command lines
PCHANGE	Changes values of material constants, as required
DISPATCH	Interprets command lines
RMATL	Reads material properties file
SMATL	Sets variables for material properties
INTTEMP	Interpolates material properties with respect to temperature
RUNOUT	Interprets OUTPUT command
OUTPUTI	Initialises output files
OUTPUTC	Closes an output file
OUTPUTR	Re-zones an output file
OUTPUTA	Appends a file to an output file
PERTURB	Processes PERTURB command by looping through material properties
STORE	Stores values of state variables
RESTORE	Restores stored values of state variables
RUNSOLVE	Supplies initial conditions to the solver
LOADUSE	Calculates current 'load'
SOLVE	Sets parameters for the Livermore Solver
LSODE	Livermore Solver for systems of Ordinary Differential Equations
DYDT	Calculates state variable derivatives for LSODE
CONLOAD	Calculates stress, total strain and elastic strain
EFFRAT	Calculates equivalent inelastic strain rate
EFFSTR	Calculates effective stress
CALCK2	Calculates K2 for inelastic strain rate equations
CALCWRK	Calculates inelastic work rate
INTDY	Interpolates derivatives of state variables (part of Livermore Solver)
OUTPUTW	Writes to the output file

Figure A.1 FORTRAN routines in unified constitutive model standalone program TREACLE.

```
TREACLE
   | INITIAL
   | INTERP
      | PCHANGE
         | DISPATCH
            | RMATL
            | SMATL
            |    | INTTEMP
            | RUNOUT
            |    | OUTPUTI
            |    | OUTPUTC
            |    | OUTPUTR
            |    | OUTPUTA
            | PERTURB
            |    | INTERP
            | RESTORE
            | STORE
            | RUNSOLVE
               | LOADUSE
               | INTTEMP
               | SOLVE
                  | LSODE*
                  |    | DYDT
                  |    |    | LOADUSE
                  |    |    | INTTEMP
                  |    |    | CONLOAD
                  |    |    | EFFRAT
                  |    |    | EFFSTR
                  |    |    | CALCK2
                  |    |    | EFFRAT
                  |    |    | CALCWRK
                  | LOADUSE
                  | INTTEMP
                  | CONLOAD
                  | INTDY**
                  | EFFRAT
                  | EFFSTR
                  | CALCWRK
                  | OUTPUTW
```

Figure A.2 Sequence of routines for unified constitutive model standalone program TREACLE

* LSODE is the top-level routine of the Livermore Solver for ODEs. Its call structure is not shown here, except for DYDT, which is a user-supplied subroutine.

** INTDY is part of the Livermore Solver, but here it is called independently

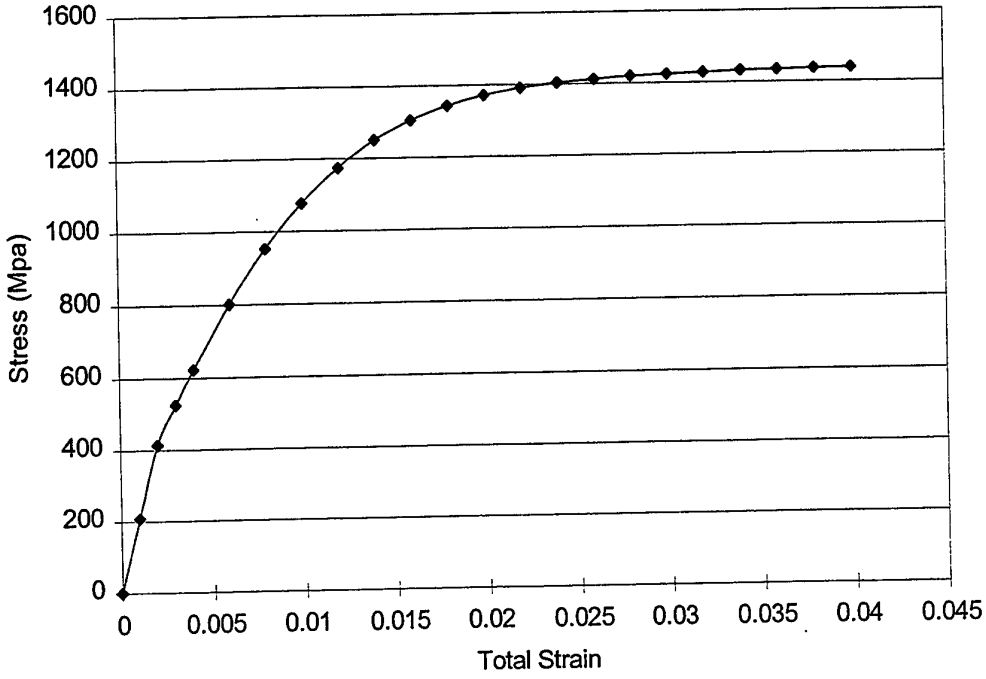

Figure 1. Uniaxial stress-strain curve for material used in test cases (data points generated by TREACLE).

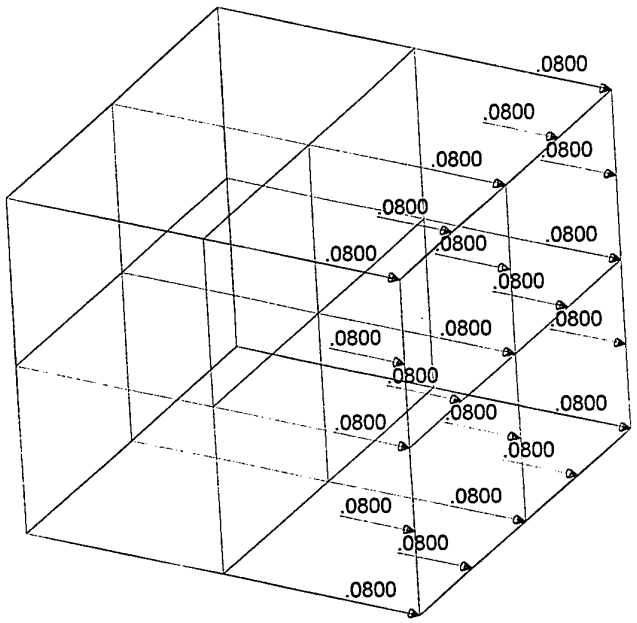

Figure 2a. Finite element mesh with maximum prescribed displacements (mm) for test cases 1 and 4.

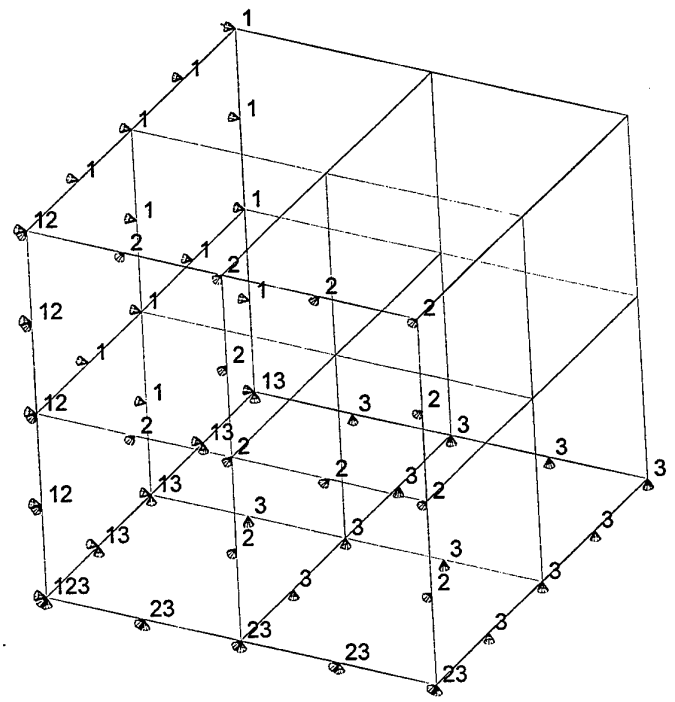

Figure 2b. Finite element mesh with directional restraints for test cases 1 and 4.

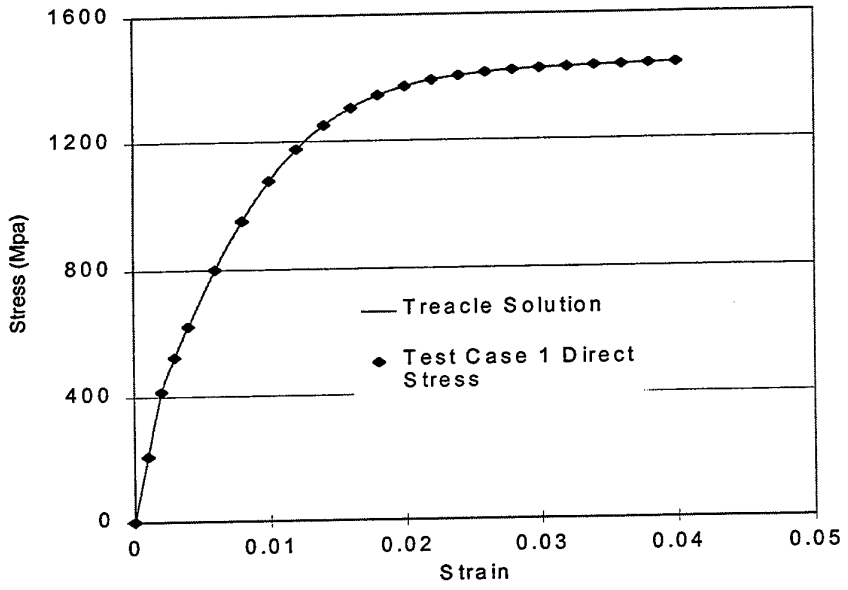

Figure 3. Results of test case 1 compared to validation solution.

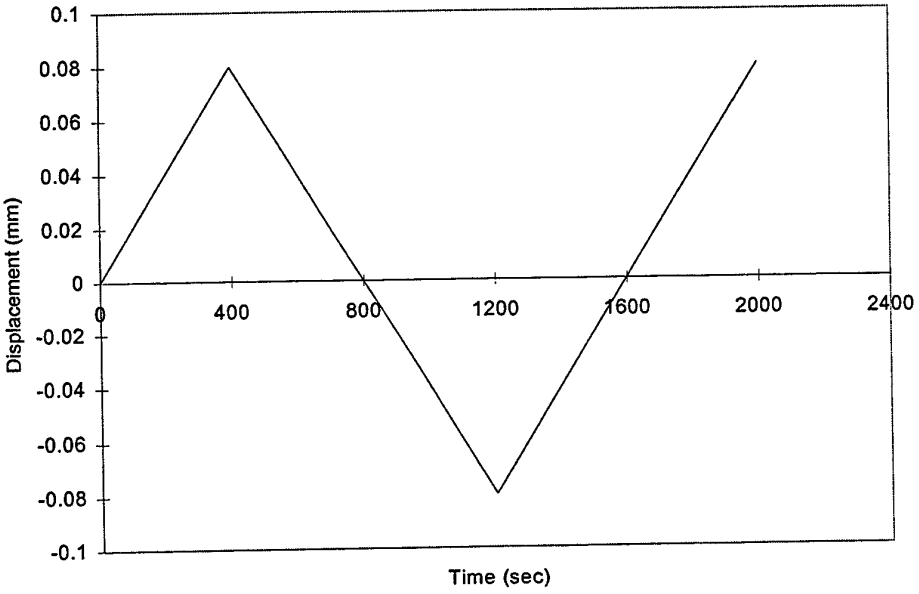

Figure 4. History of prescribed displacements (mm) for test case 4.

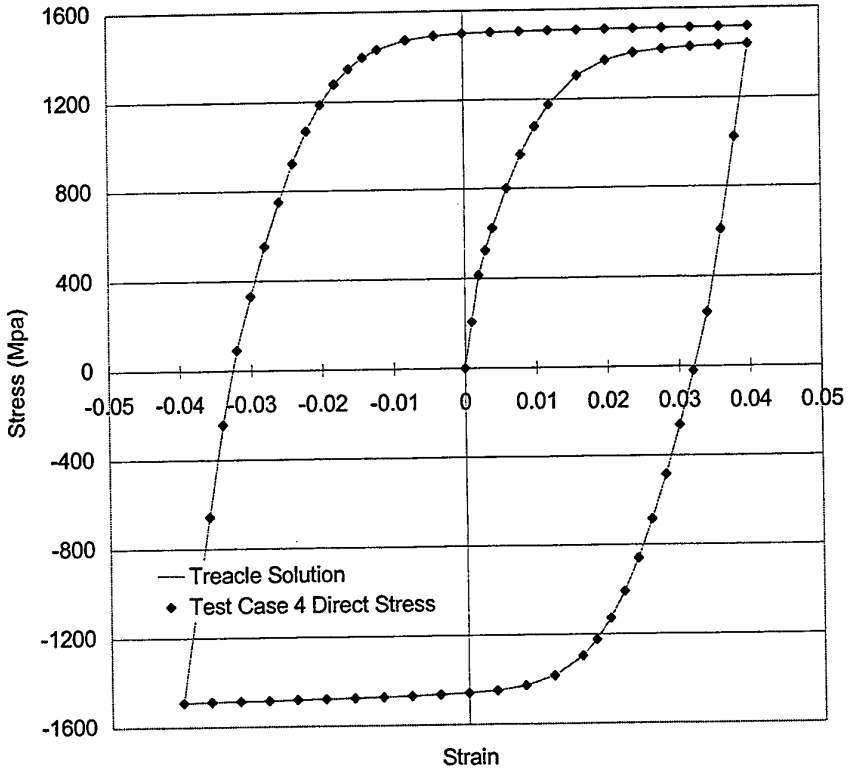

Figure 5. Results of test case 4 compared to validation solution.

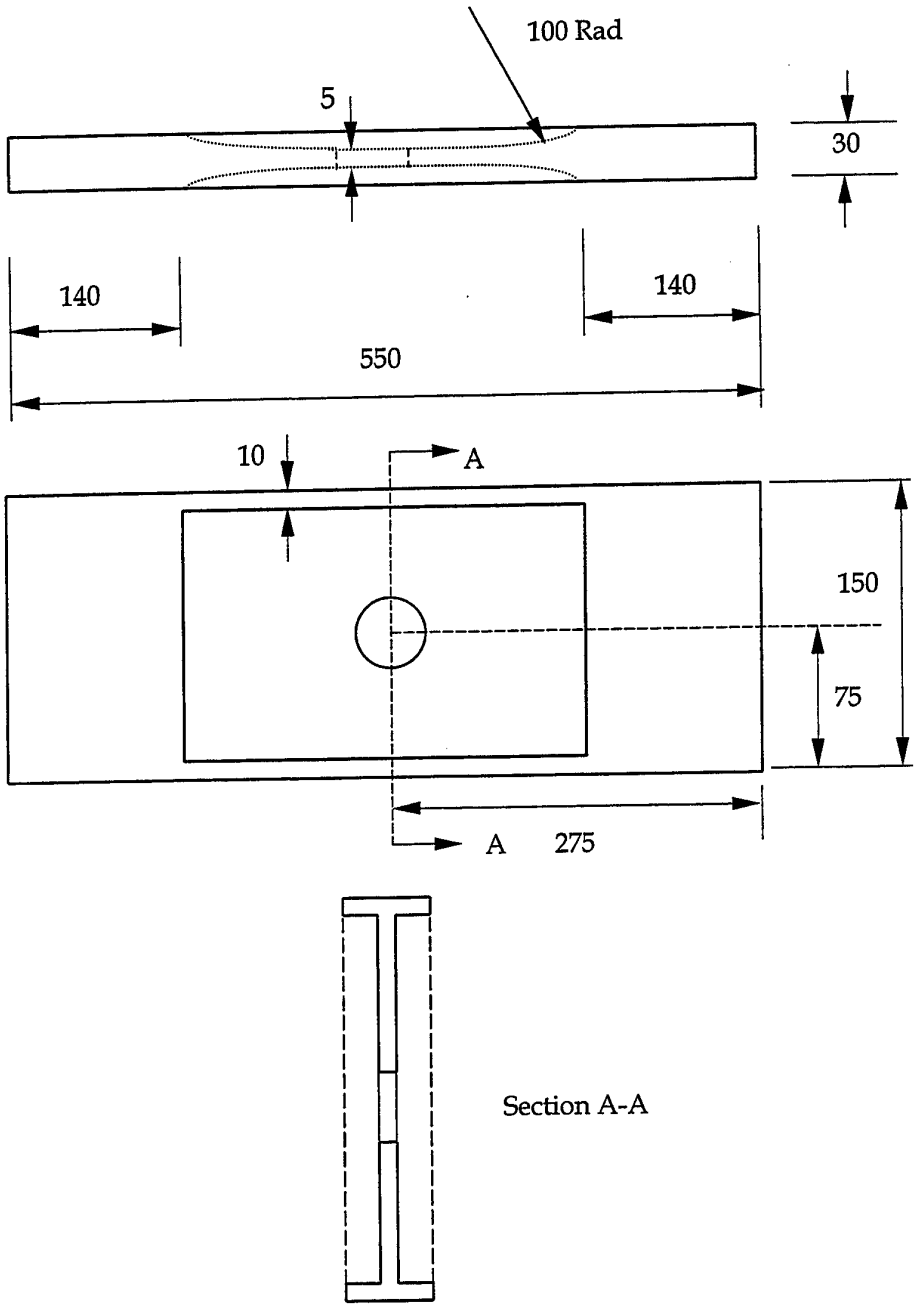

Figure 6. Dimensions (mm) of I-beam test specimen (not to scale).

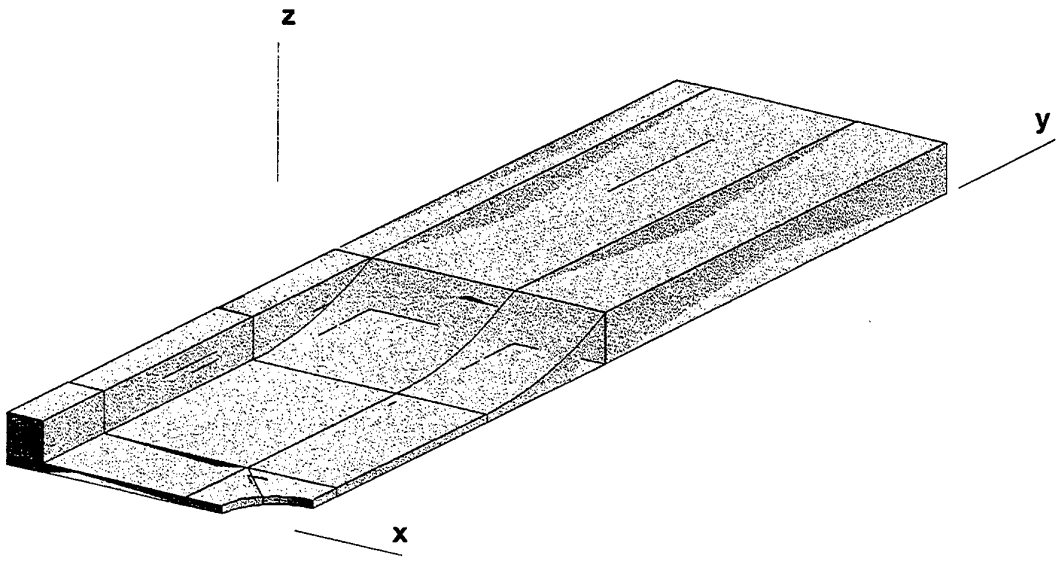

Figure 7. Finite element blocking scheme for I-beam test specimen (1/8 model).

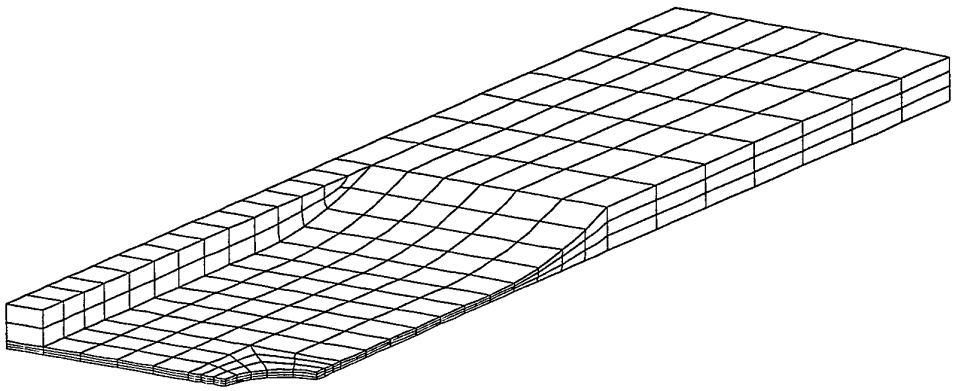

(a) overall

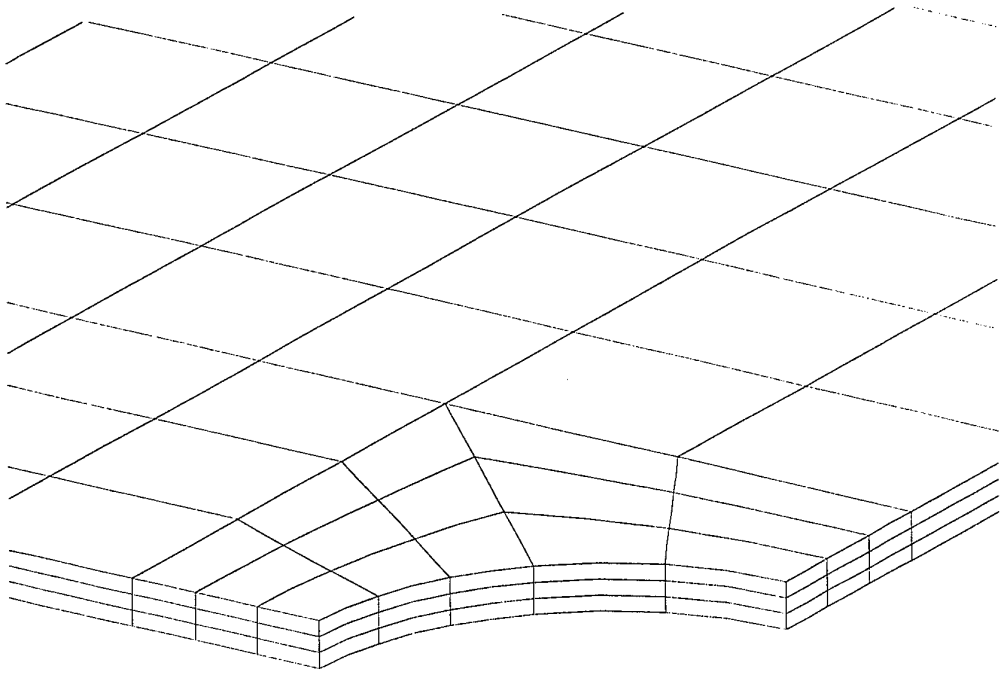

(b) around hole

Figure 8. Initial coarse finite element mesh for I-beam test specimen.

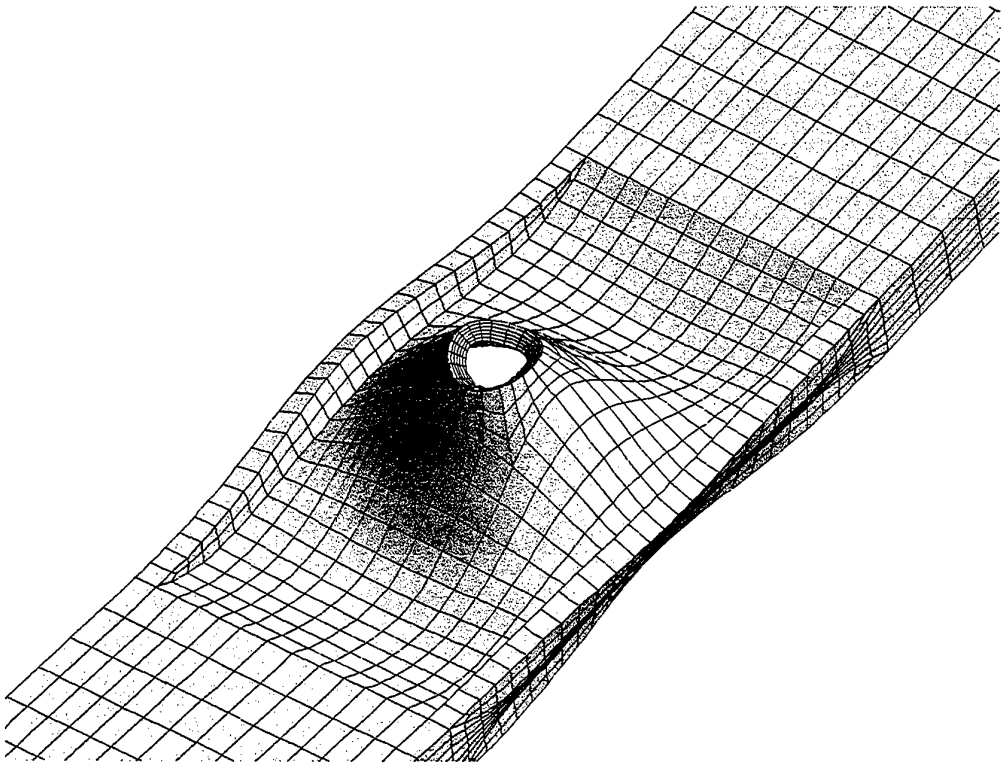

Figure 9. Predicted critical buckling mode of I-beam test specimen.

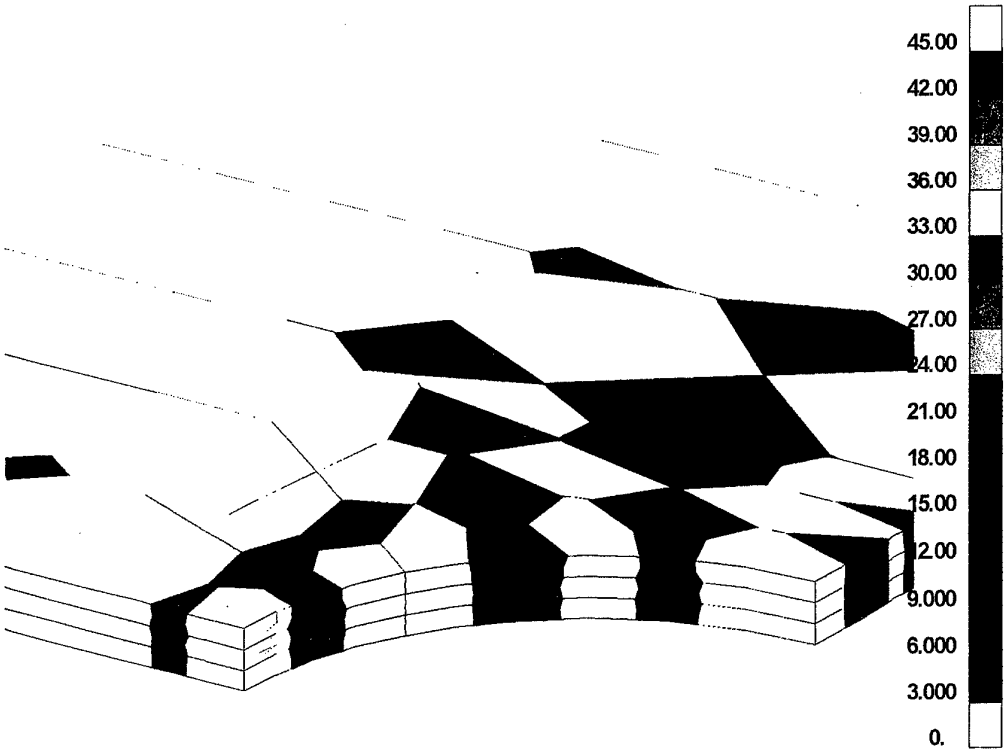

Figure 10. Stress mismatch between element predictions at common nodes (MPa) - initial coarse finite element mesh (1/8 model).

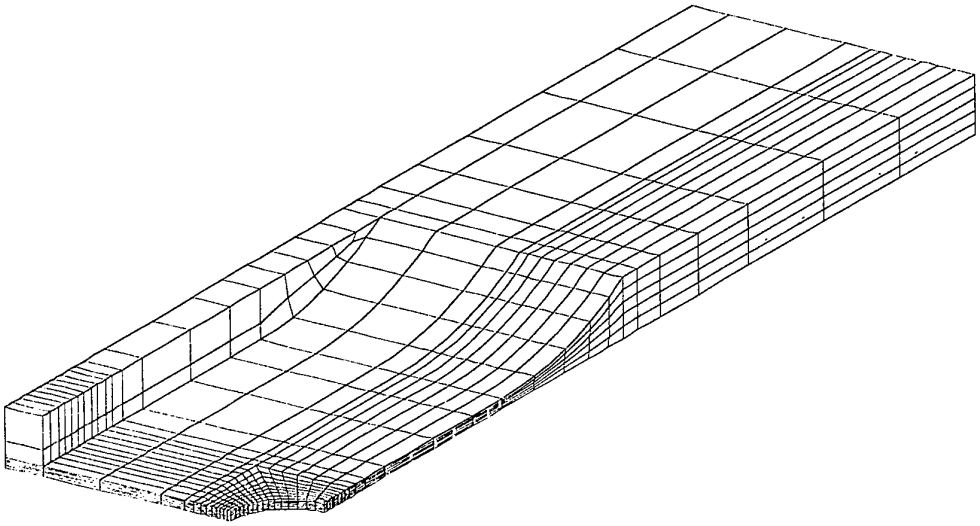

(a) overall

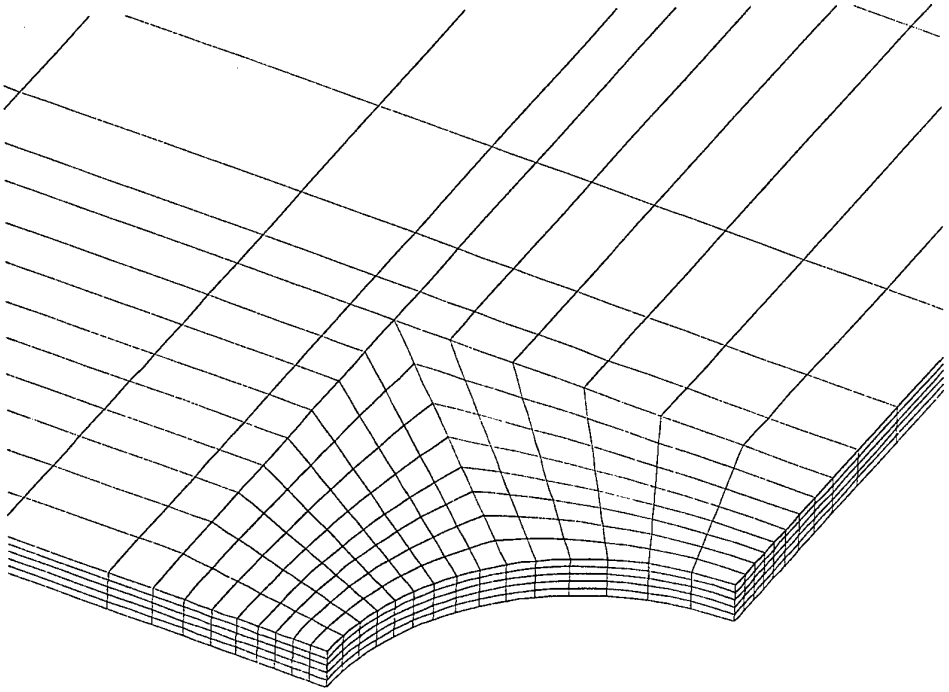

(b) around hole

Figure 11. Refined finite element mesh for test specimen.

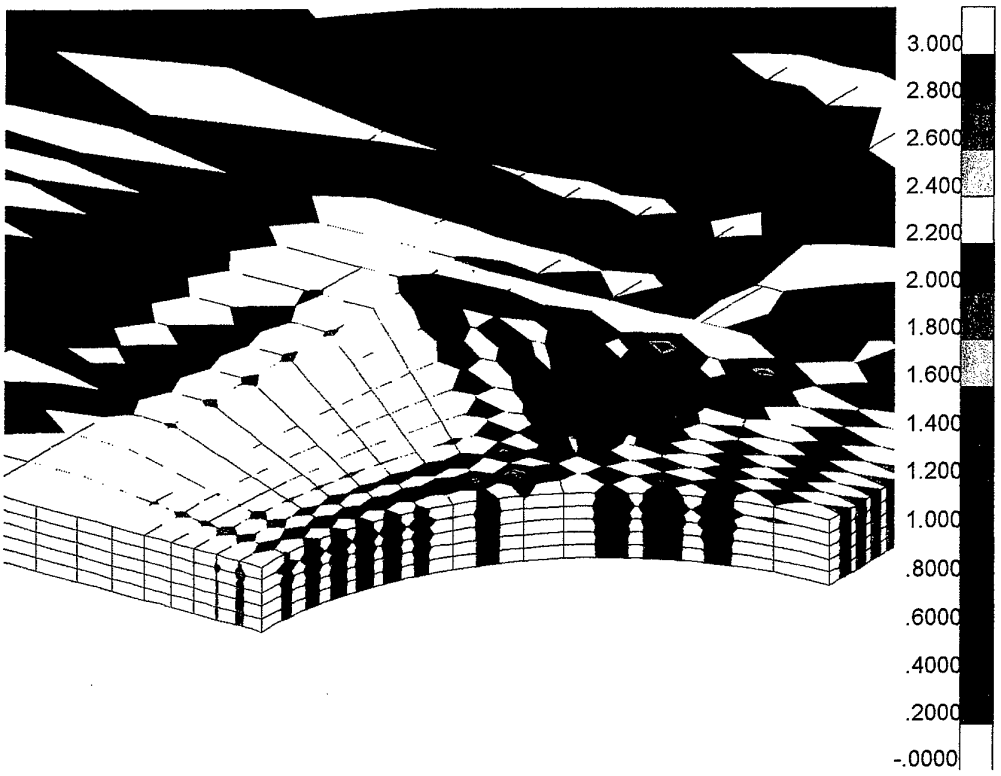

Figure 12. Stress mismatch between element predictions at common nodes (MPa) - refined finite element mesh (1/8 model).

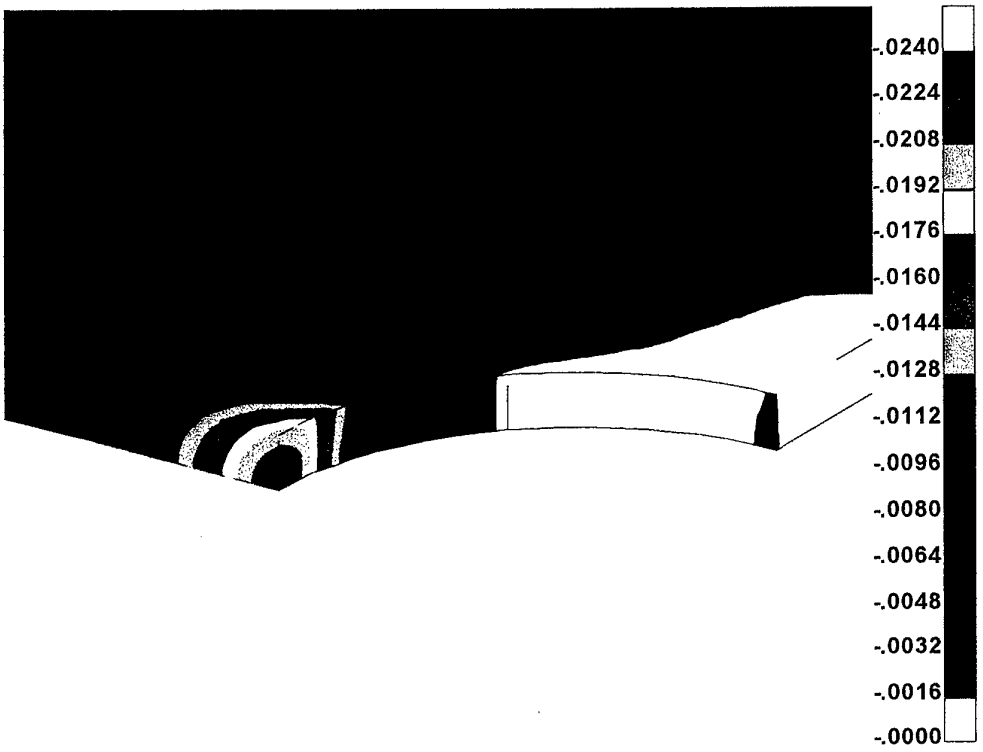

Figure 13. Total longitudinal strain (ε_{yy}) at compressive load of 1012 kN using classical plasticity.

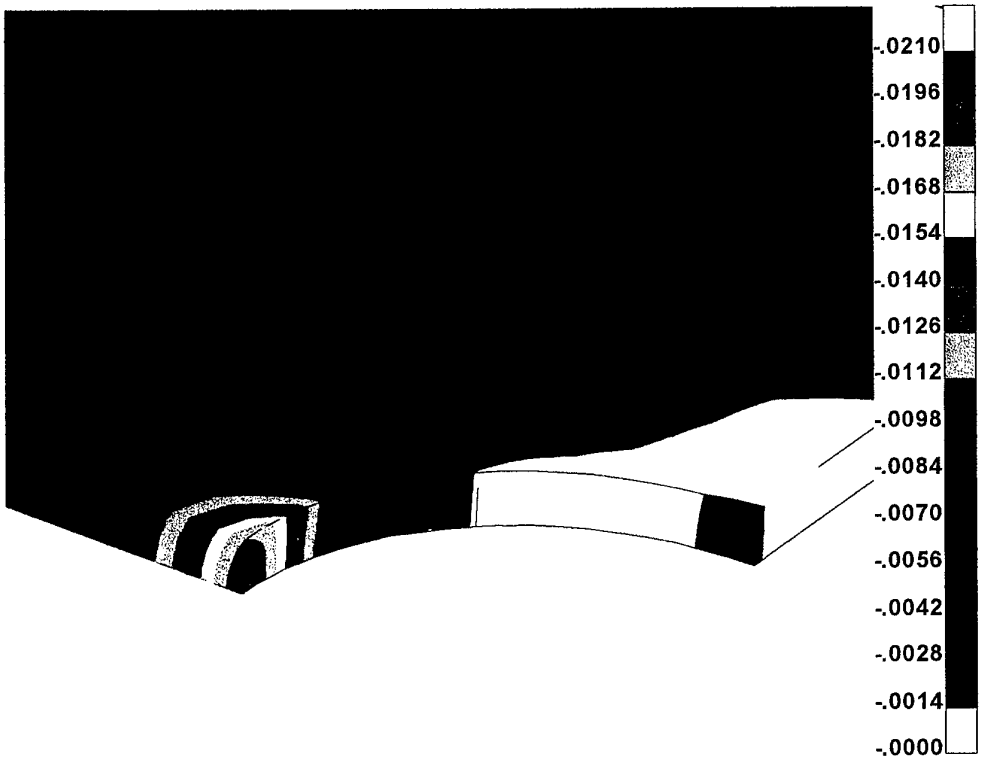

Figure 14. Total longitudinal strain (ε_{yy}) at compressive load of 1012 kN using unified constitutive model.

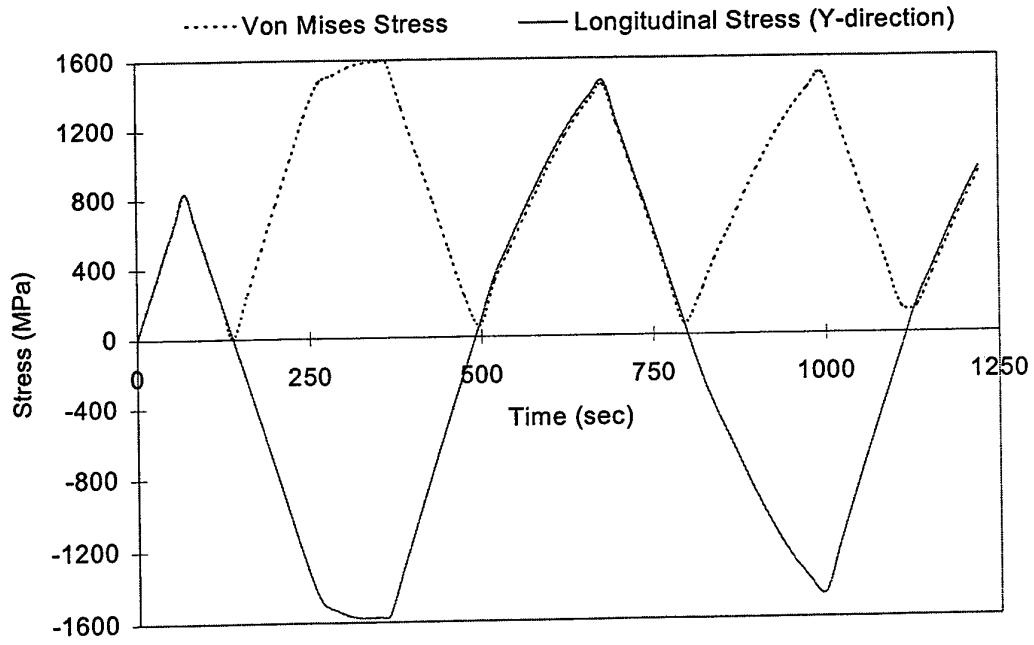

Figure 15. A finite element stress history predicted by unified constitutive model at critical location for CPLT loading.

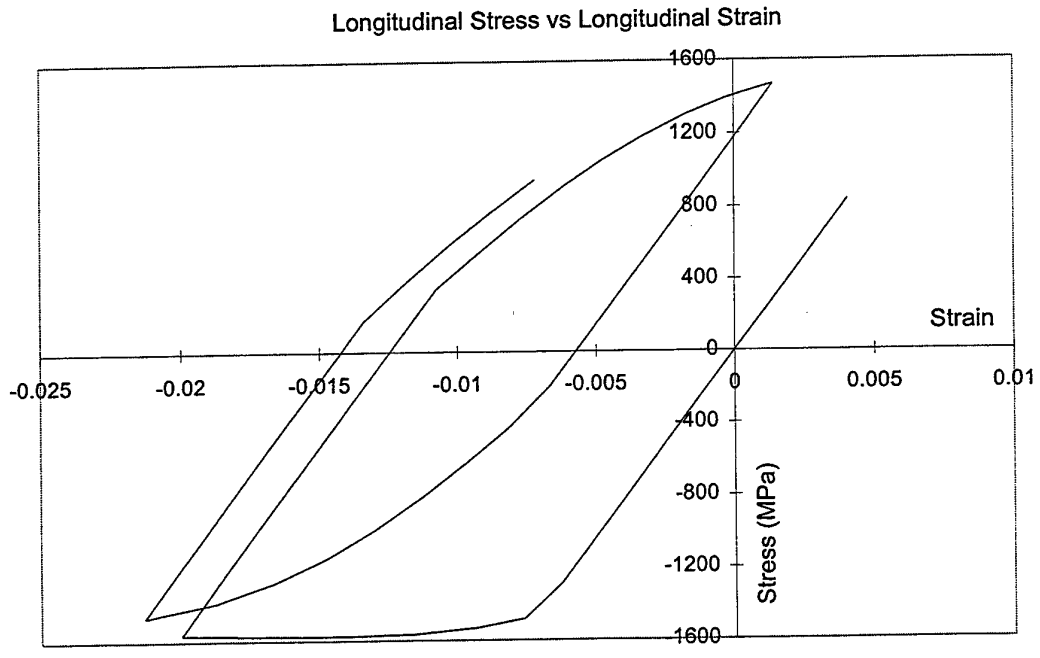

Figure 16. Longitudinal stress vs strain predicted by unified constitutive model at critical location for CPLT loading.

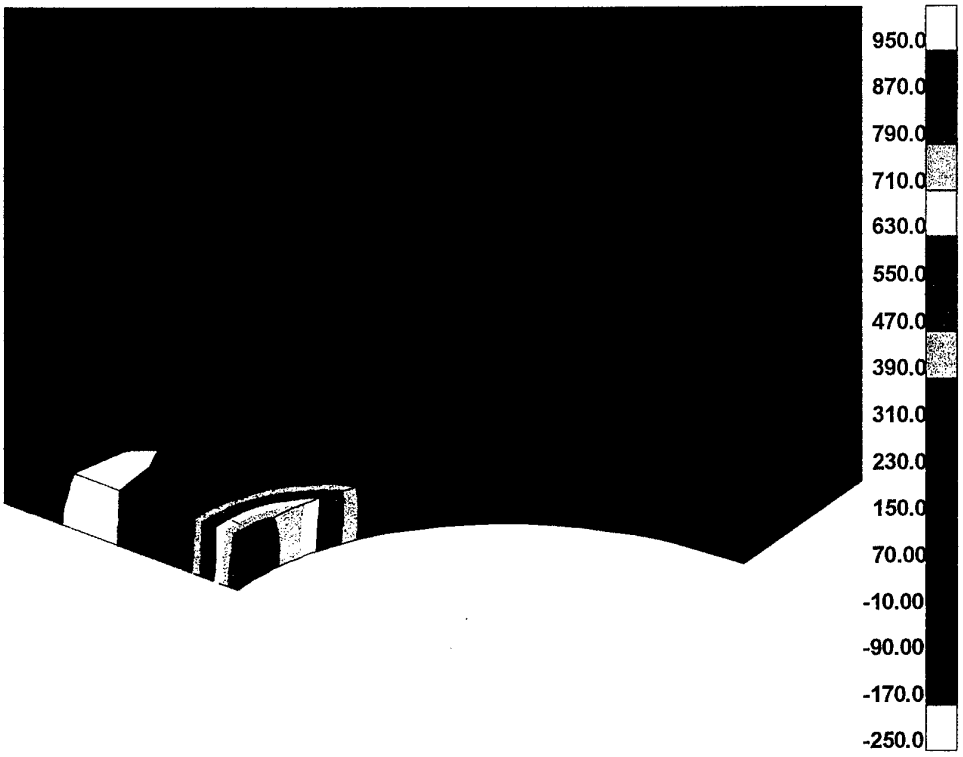

Figure 17. Residual longitudinal stress distribution (σ_{yy}, MPa) at completion of 1st CPLT cycle

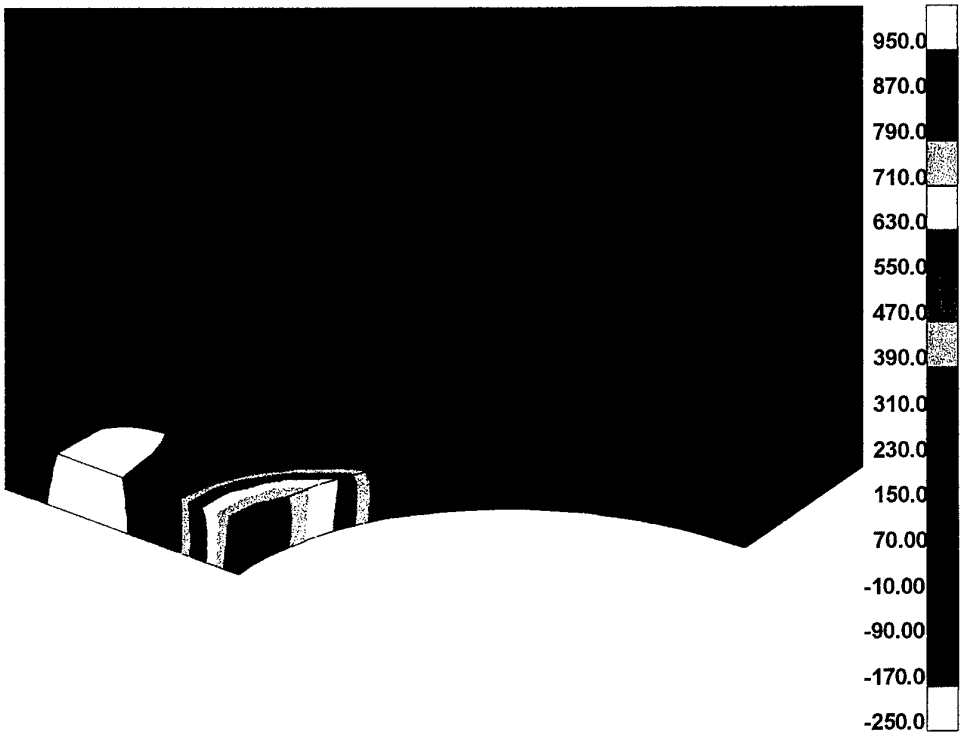

Figure 18. Residual longitudinal stress distribution (σ_{yy}, MPa) at completion of 2nd CPLT cycle

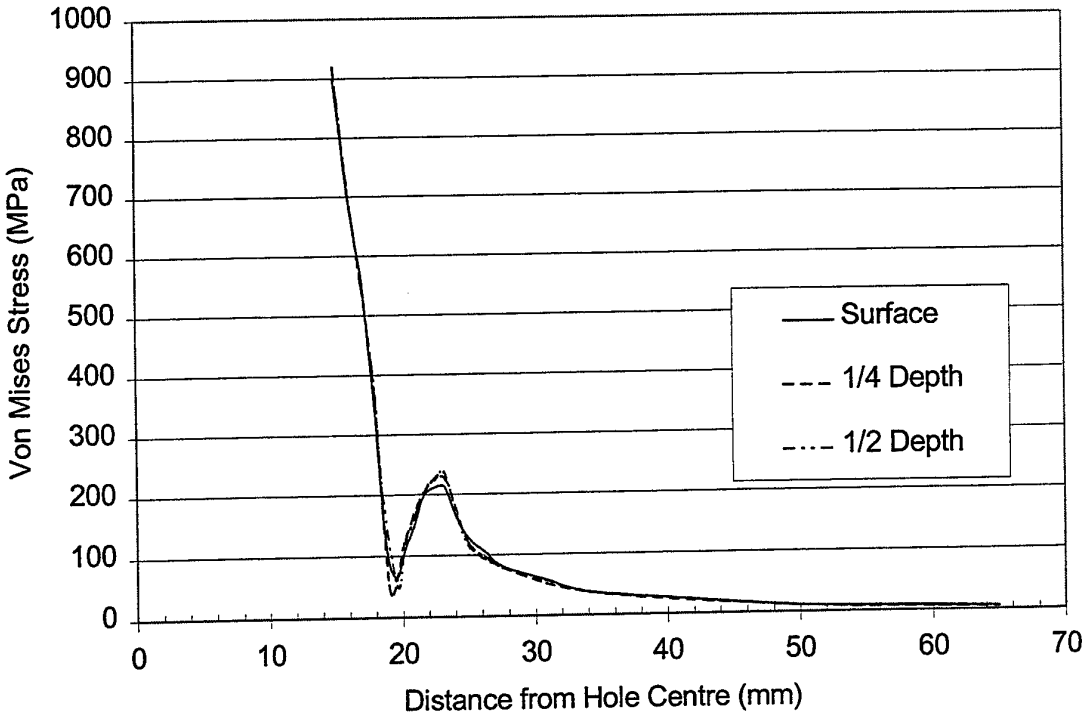

(a) Full range

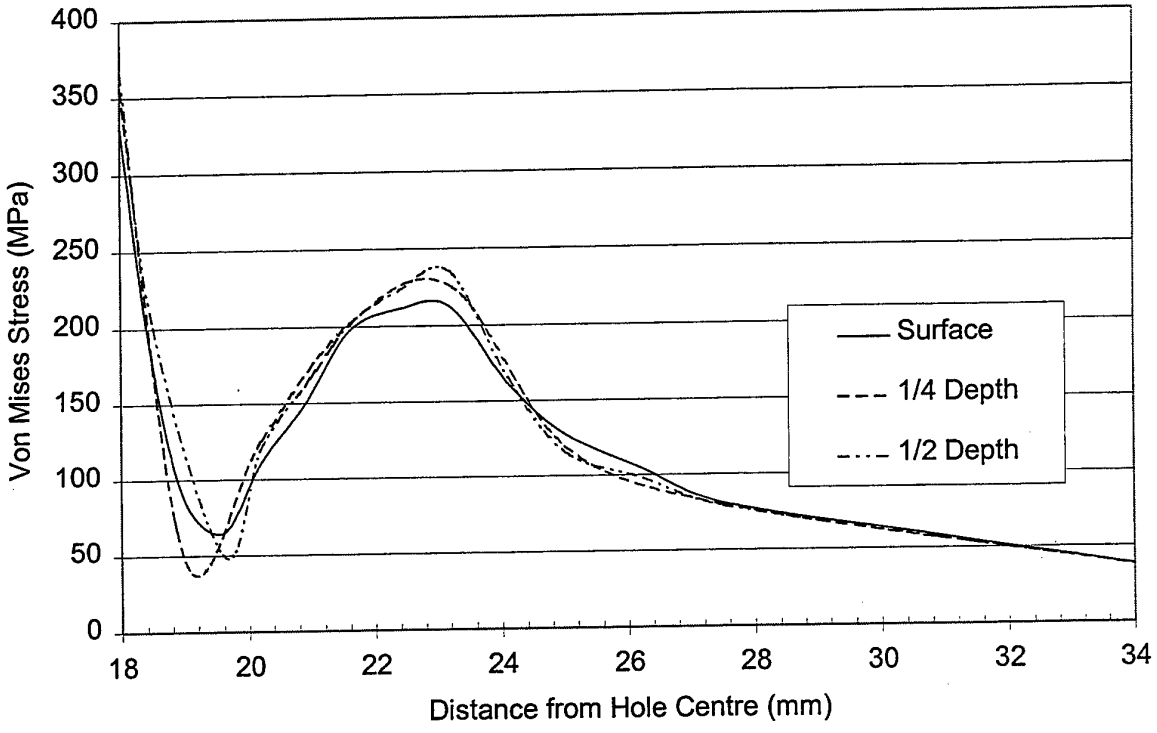

(b) Detail near local minima and maxima

Figure 19. Residual Von Mises stress distribution (MPa) along half-width of the specimen at completion of 2nd CPLT cycle

DISTRIBUTION LIST
Implementation of a Unified Constitutive Model into the
ABAQUS Finite Element Package

R.J.Wescott, K.C.Watters and M.Heller

AUSTRALIA

DEFENCE ORGANISATION

Task Sponsor
DTA-LC
S&T Program
Chief Defence Scientist
FAS Science Policy
AS Science Corporate Management
} shared copy
Director General Science Policy Development
Counsellor Defence Science, London (Doc Data Sheet)
Counsellor Defence Science, Washington (Doc Data Sheet)
Scientific Adviser to MRDC Thailand (Doc Data Sheet)
Scientific Adviser Policy and Command
Navy Scientific Adviser (Doc Data Sheet and distribution list only)
Scientific Adviser - Army (Doc Data Sheet and distribution list only)
Air Force Scientific Adviser
Director Trials

Aeronautical and Maritime Research Laboratory
Director
Chief of Airframes and Engines Division
Research Leader, Fracture Mechanics
B.Wicks
R. Callinan
C.Wang
C.Quan
M.Burchill
J. Hou
W. Waldman
Author(s): R.Wescott (5 copies)
K.Watters (5 copies)
M.Heller (7 copies)

DSTO Library and Archives
Library Fishermans Bend
Library Maribyrnong
Library Salisbury (2 copies)
Australian Archives
Library, MOD, Pyrmont (Doc Data sheet only)
*US Defense Technical Information Center, 2 copies
*UK Defence Research Information Centre, 2 copies
*Canada Defence Scientific Information Service, 1 copy
*NZ Defence Information Centre, 1 copy
National Library of Australia, 1 copy

Capability Development Division
Director General Maritime Development (Doc Data Sheet only)
Director General Land Development (Doc Data Sheet only)
Director General C3I Development (Doc Data Sheet only)
Director General Aerospace Development

Army
ABCA Standardisation Officer, Puckapunyal, (4 copies)
SO (Science), DJFHQ(L), MILPO Enoggera, Queensland 4051 (Doc Data Sheet only)
NAPOC QWG Engineer NBCD c/- DENGRS-A, HQ Engineer Centre Liverpool Military Area, NSW 2174 (Doc Data Sheet only)

Air Force
ASI2A

Intelligence Program
DGSTA Defence Intelligence Organisation

Corporate Support Program
OIC TRS, Defence Regional Library, Canberra

UNIVERSITIES AND COLLEGES
Australian Defence Force Academy
Library
Head of Aerospace and Mechanical Engineering
Serials Section (M list), Deakin University Library, Geelong, 3217
Senior Librarian, Hargrave Library, Monash University
Librarian, Flinders University

OTHER ORGANISATIONS
NASA (Canberra)
AGPS

OUTSIDE AUSTRALIA

ABSTRACTING AND INFORMATION ORGANISATIONS
Library, Chemical Abstracts Reference Service
Engineering Societies Library, US
Materials Information, Cambridge Scientific Abstracts, US
Documents Librarian, The Center for Research Libraries, US

INFORMATION EXCHANGE AGREEMENT PARTNERS
Acquisitions Unit, Science Reference and Information Service, UK
Library - Exchange Desk, National Institute of Standards and Technology, US
National Aerospace Laboratory, Japan (
National Aerospace Laboratory, Netherlands
SPARES (5 copies)

Total number of copies: 74

DEFENCE SCIENCE AND TECHNOLOGY ORGANISATION
DOCUMENT CONTROL DATA

1. PRIVACY MARKING/CAVEAT (OF DOCUMENT)

2. TITLE

Implementation of a Unified Constitutive Model into the ABAQUS Finite Element Package

3. SECURITY CLASSIFICATION (FOR UNCLASSIFIED REPORTS THAT ARE LIMITED RELEASE USE (L) NEXT TO DOCUMENT CLASSIFICATION)

Document	(U)
Title	(U)
Abstract	(U)

4. AUTHOR(S)

R.J. Wescott, K.C. Watters and M. Heller

5. CORPORATE AUTHOR

Aeronautical and Maritime Research Laboratory
PO Box 4331
Melbourne Vic 3001 Australia

6a. DSTO NUMBER	6b. AR NUMBER	6c. TYPE OF REPORT	7. DOCUMENT DATE
DSTO-TR-0833	AR-011-003	Technical Report	June 1999

8. FILE NUMBER	9. TASK NUMBER	10. TASK SPONSOR	11. NO. OF PAGES	12. NO. OF REFERENCES
M1/8/1161	96/102	DTA-LC	34	9

13. DOWNGRADING/DELIMITING INSTRUCTIONS

14. RELEASE AUTHORITY

Chief, Airframes and Engines Division

15. SECONDARY RELEASE STATEMENT OF THIS DOCUMENT

Approved for public release

OVERSEAS ENQUIRIES OUTSIDE STATED LIMITATIONS SHOULD BE REFERRED THROUGH DOCUMENT EXCHANGE, PO BOX 1500, SALISBURY, SA 5108

16. DELIBERATE ANNOUNCEMENT

No Limitations

17. CASUAL ANNOUNCEMENT Yes

18. DEFTEST DESCRIPTORS

F-111 Aircraft; Plastic Deformation; Stress Analysis; Finite Element Method; Residual Stress;

19. ABSTRACT

Unified constitutive models have previously been developed at AMRL and implemented into the PAFEC and ABAQUS Finite Element packages to predict the stress-strain response of structures that undergo multi-axial, rate dependent, cyclic plasticity. In this work, the ABAQUS version of the model has been enhanced to account for advances in unified constitutive modelling, and for consistency with the existing PAFEC version of the model. Numerous test cases have been run to validate the model's implementation in ABAQUS. A full 3-dimensional analysis of a proposed test specimen has been undertaken to study residual stress distribution with the ultimate goal of helping to manage fatigue crack growth in the F-111 aircraft.